AIAA SciTech Forum
8-12 January 2024, Orlando, FL
AIAA SCITECH 2024 Forum

10.2514/6.2024-1708

AI-Driven Multidisciplinary Conceptual Design of Unmanned Aerial Vehicles

Hasan Karali *, Gokhan Inalhan † and Antonios Tsourdos ‡
Cranfield University, MK43 0AL, United Kingdom

This paper presents a multidisciplinary conceptual design framework for unmanned aerial vehicles based on artificial intelligence-driven analysis models. This approach leverages AI-driven analysis models that include aerodynamics, structural mass, and radar cross-section predictions to bring quantitative data to the initial design stage, enabling the selection of the most appropriate configuration from various optimized concept designs. Due to the design optimization cycle, the initial dimensions of key components such as the wing, tail, and fuselage are provided more accurately for later design activities. Simultaneously, the generated structure enables more suitable design point selection through the feedback loop within the design iteration. Therefore, in addition to reducing design costs, this approach also offers a substantial time advantage in the overall design process.

I. Introduction

The design process, specifically for unmanned aerial vehicles, involves certain differences. Particularly when addressing unmanned aerial vehicle concepts, all considerations and constraints related to pilots and crew are eliminated in the design process. In today's context, autonomous control systems, new manufacturing techniques, and material technologies compel a reevaluation of the design process in a completely different manner. If operational requirements are taken into account, the situation becomes even more complex. The pursuit of cost-effective UAVs in today's context is driven by the need to optimize operational efficiency, minimize risks, and provide diverse mission requirements while accommodating advancements in technology and market demands. In this sense, systems that utilize common components and enable rapid and cost-effective production come to the forefront. A key challenge lies in developing design approaches that incorporate non-conventional perspectives, particularly in the next-generation design of "plug & play" configurations across a fleet of unmanned combat aerial vehicles (UCAVs) [1–3]. These vehicles are expected to provide challenging mission requirements and specific system designs, emphasizing the minimization of full life-cycle costs [4–9]. For example, a combat mission might require a smaller span wing with a reduced radar cross-section area, whereas an ISR mission might necessitate larger wings to accommodate heavier payloads for extended durations. Identifying the most suitable components for each mission scenario involves navigating through various optimum points in an extensive design space.

In the situation mentioned above, as in the case of UAVs, the design process often necessitates the integration of various engineering disciplines. The multidisciplinary design optimization approach serves to consolidate all disciplines into a unified framework. Multidisciplinary design optimization (MDO) refers to the design of complex engineering systems comprising interactive subsystems influenced by interdependent physical phenomena [10]. In aircraft design studies, the typical disciplines within MDO include aerodynamic performance, structural layout, mass and stability, and propulsion systems. As mentioned in [11], aircraft design optimization has historically utilized semi-empirical equations to swiftly analyze conventional fixed-wing aircraft. However, the application of these low-fidelity models to UAVs can pose challenges due to their reliance on traditional fixed-wing regression data. In general, the data in semi-empirical approaches are not very accurate, especially in terms of aerodynamic performance, as stated in [12], since they do not cover the dimensions and flight conditions of UAVs. Therefore, more complex approaches such as numerical methods should enter the design process earlier. However, performing optimization via high-fidelity tools, which need many evaluations of the mathematical model to compute the performance of the system at each iteration loop, can be computationally expensive and time consuming [13]. At this point, machine learning based solutions come to the fore in the literature as an alternative approach to this problem. Machine learning is a computational approach that enables systems to learn and improve from experience without being explicitly programmed, with a primary focus

*PhD Student, School of Aerospace, Transport and Manufacturing, hasan.karali@cranfield.ac.uk, AIAA Member
†BAE Systems Chair, Professor of Autonomous Systems and Artificial Intelligence, inalhan@cranfield.ac.uk, AIAA Associate Fellow
‡Professor, School of Aerospace, Transport and Manufacturing, a.tsourdos@cranfield.ac.uk

on exploiting data to improve performance and make informed decisions. The field of aerospace engineering, which is packed with data and already constructed on a limited multi-objective optimization framework that is perfectly suited for contemporary machine learning approaches, is perhaps the best example of the potential for data-driven advancement [14]. Particularly in terms of design optimization and upgrade analysis, performance validation and optimization, and product improvement and calibration, digital twins offer significant advantages [15]. In the literature, there are several machine learning-based studies for the conceptual/preliminary design of aerial vehicles. In [16], the study investigates configuration selection by leveraging the existing UAV database using decision tree classifiers. However, this UAV database is limited and as there is no quantitative value or performance calculation for comparison, it is inadequate like other attempts in the literature. Another major gap in the literature is that almost all of the studies are limited to certain parts of the aircraft, such as the 2D airfoil or the 3D wing [17–29]. Approximate models for aerodynamic coefficients of complete aircraft geometry used in aerodynamic shape optimization are very limited.

Especially nowadays, it is not possible to develop different concept configurations and design iterations due to the situation caused by competition and limited budgets. That is why focusing on the right concept from the beginning is crucial. However, the human interaction level is remarkably decisive in the early phase of the design process (see Fig. 1). To integrate numerical data into the design process at an early stage, we have created an intelligent conceptual design method in this work that consists of AI-driven surrogate models and optimization loops. This technique makes it feasible to evaluate the initial optimal configurations of several concepts and select the best fit. Thus, using a toolset that is computationally quick, low-cost, and of a higher order than current approaches, the selection of the concept configuration satisfies the design requirements. At the same time, the initial sizing and the design iteration are all automated, lowering the amount of human engagement.

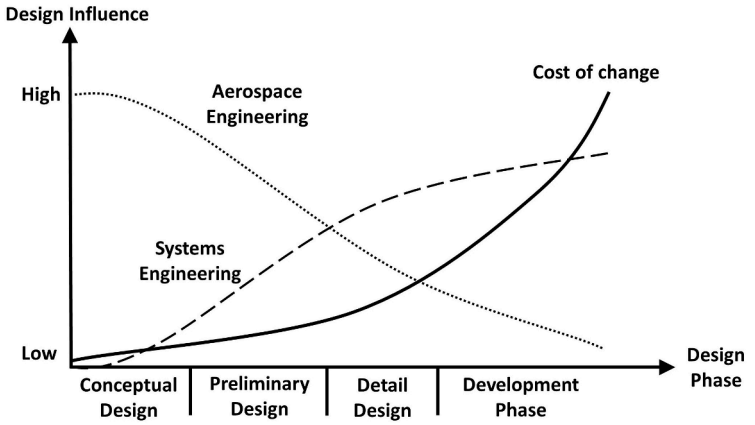

Fig. 1 Design influence and the cost of change in the design phase

The rest of the paper is organized as follows: In the “Methodology” section, the main algorithm of the paper is briefly given. This section includes "Design Point Calculation", "Initial Sizing Algorithm", "Aircraft Model", "AI-based Surrogate Models", and "Multi-Objective Genetic Algorithm" subsections. In the "Application of the Model" section, an example application of the developed model is performed. Finally, the achieved objectives are presented in the "Conclusion" part.

II. Methodology

The AI-driven conceptual design algorithm consists of four main parts: Design Point Calculation, Initial Sizing, AI-driven Aircraft Model, and Optimization of Configurations. Each part is connected to another through an input-output relationship. Additionally, the design iteration loop added to the algorithm enabled more accurate designs to be obtained. Figure 2 represents the general structure of the algorithm.

The method starts with giving the design requirements to the algorithm. These requirements may include performance requirements such as maximum take-off weight, payload weight, cruise altitude-speed, or restrictions about configuration dimensions. Then, wing loading and thrust loading values that will meet these performance requirements are calculated using the design point calculation. The initial sizing algorithm takes these values and calculates the basic dimensions along with the initial requirements. These are the wing area, length, and hydraulic diameter of the fuselage. Afterward,

configurations that will maximize performance while meeting the requirements are searched in the design space with the help of the optimization algorithm. Since the aircraft models used here are AI-driven surrogate models, it is possible to search the design space in a very flexible way.

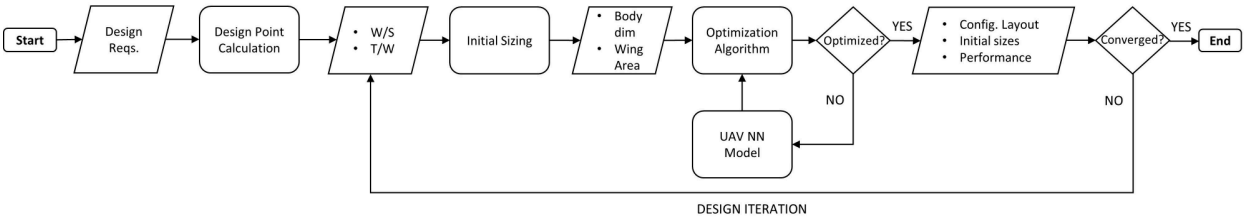

Fig. 2 General overview of the proposed framework

A. Design Point Calculation

In design point calculation, given performance requirements such as stall speed (V_s), maximum speed (V_{max}), maximum rate of climb (ROC_{max}), take-off run (S_{TO}), ceiling (h_c) are used to determine a feasible design space in terms of wing loading (W/S) and thrust loading (T/W). To determine the optimum selection the flight performance equations are solved based on wing loading and thrust loading, and inequality restrictions are generated as a result. This approach is entirely dependent on the aircraft's performance requirements and makes use of flight mechanics theory. As a result, the procedure is an analytical approach, and the outcomes are highly trustworthy.

The wing loading based on stall speed requirements is shown as:

$$\left(\frac{W}{S}\right)_{V_s} = \frac{1}{2}\rho V_s^2 C_{L_{max}} \tag{1}$$

where ρ denotes the air density and $C_{L_{max}}$ is the aircraft maximum lift coefficient. The following relation is used for the maximum speed requirement:

$$\left(\frac{T_{SL}}{W}\right)_{V_{max}} = \rho_o V_{max}^2 C_{D_o} \frac{1}{2\left(\frac{W}{S}\right)} + \frac{2K}{\rho\sigma V_{max}^2}\left(\frac{W}{S}\right) \tag{2}$$

where ρ_o is the sea-level air density, C_{D_o} is the zero-lift drag coefficient and K is referred to as the induced drag factor.

$$\left(\frac{T}{W}\right)_{S_{TO}} = \frac{\mu - \left(\mu + \frac{C_{D_G}}{C_{L_R}}\right)\left[\exp\left(0.6\rho g C_{D_G} S_{TO}\frac{1}{W/S}\right)\right]}{1 - \exp\left(0.6\rho g C_{D_G} S_{TO}\frac{1}{W/S}\right)} \tag{3}$$

where μ is runway surface friction coefficient and is generally taken as 0.05 for concrete/asphalt surfaces. C_{L_R} represents the aircraft lift coefficient at take-off rotation. It can be obtained by solving the lift equation inversely using take-off rotation speed ($1.1 - 1.2V_s$). The wing and engine sizing based on rate of climb requirements can be defined as follows:

$$\left(\frac{T}{W}\right)_{ROC} = \frac{ROC}{\sqrt{\frac{2}{\rho\sqrt{\frac{C_{D_0}}{K}}}\left(\frac{W}{S}\right)}} + \frac{1}{(L/D)_{max}} \tag{4}$$

The ceiling is defined as the highest altitude at which an aircraft maintains its level flight. The ceiling is not a critical requirement for many aircraft, but it is critical for some missions, such as ISR (Intelligence, surveillance, and reconnaissance). Similarly, as a function of wing and thrust loading, the performance equation can be stated as follows:

$$\left(\frac{T}{W}\right)_{h_C} = \frac{ROC_C}{\sigma_C\sqrt{\frac{2}{\rho_C\sqrt{\frac{C_{D_o}K}{K}}}\left(\frac{W}{S}\right)}} + \frac{1}{\sigma_C(L/D)_{max}} \tag{5}$$

The details of the relevant equations can be found in an aircraft design or flight performance book [30, 31]. To drive this process, the table-based aerodynamic and geometry parameters are used in the first design iteration. However, in the design iteration step, this information is obtained directly from the aerodynamic performance and geometry of the previous configuration.

B. Initial Sizing Algorithm

In the initial sizing step, the basic dimensions of the aircraft are calculated using the design point output and some requirements. By dividing the aircraft's maximum take-off weight by the wing loading, the wing area is computed. By multiplying the aircraft's maximum take-off weight by the thrust loading, the engine thrust is computed. Thus, the required wing area and engine thrust are obtained as follows:

$$S = W_{\text{mtow}} / \left(\frac{W}{S}\right), \quad T = W_{\text{mtow}} \cdot \left(\frac{T}{W}\right) \tag{6}$$

Engine selection is generally - in almost most cases - made among the available engines. UAV-specific engine development is not the first option due to cost and time factors. The selection of the engine, beyond numerical evaluations, also depends on several conditions such as the manufacturing country, production maintenance competence, usage permit, etc. Therefore, the current algorithm leaves it up to the user to use one of the engines that provides the required thrust level. Table 1 lists some of the available turbofan engines that can be used for example high subsonic UAV. In addition to these data, it is possible to choose an engine by taking into account specific full consumption and cost.

Table 1 Sample engine table for high subsonic UAV case

Engine	Length (mm)	Diameter (mm)	Dry Weight (kg)	Maximum Thrust (kN)
Williams FJ33	976	466	140	8.21
Pratt Whitney Canada PW617	1360	750	172	8.41
GE Honda HF120	1510	660	211.3	9.1
Pratt Whitney Canada JT15D	1531	685.8	285.7	13.57
Williams FJ44-4	1340	640	298	16.0
Ivchenko AI-25TL	3358	611.6	350	16.9
Pratt Whitney Canada 545B	1742	693.4	376.5	17.58

The length and diameter obtained after engine selection are important for aft-body sizing. There is also a mid-body length calculated based on internal payload requirements. All this data is used to determine a representative body length and diameter.

C. Aircraft Model

The aircraft model represents the main structure that includes various sub-disciplines. These sub-disciplines can be summarized as follows: Aerodynamic Model, Structural Mass Model, and Radar Cross Section Model. The aircraft model is shaped around the NASA open-source parametric geometry model, Vehicle Sketch Pad (OpenVSP), which allows the user to create three-dimensional parametric models of generic aircraft configurations defined by common engineering parameters [32]. The ability of OpenVSP to swiftly and practically construct a solid model and export/use this geometry in various formats is extremely useful in conceptual and preliminary design processes [33, 34]. In this study, OpenVSP - Python API integration was preferred, which provides coding flexibility to connect the algorithm to the other disciplines.

1. Aerodynamic Model

Determining aerodynamic characteristics at the conceptual/preliminary design stages is predominant for the successful development of UAVs. At these early phases of design, critical decisions are made that significantly impact the entire development process. Understanding the aerodynamics of a UAV is crucial for achieving optimal performance,

efficiency, and mission success. By assessing aerodynamic characteristics early on, designers can make informed decisions about wing configurations, airfoil selections, and overall vehicle layout.

By making some assumptions about flow conditions and geometry, low-order aerodynamic models can forecast aircraft performance inexpensively and rapidly. Although one of the well-known computational aerodynamics approaches, potential flow-based panel methods, provides more complicated geometry modeling and solutions than semi-empirical, lifting line, and vortex lattice methods (VLM), it remains at a lesser level when compared to CFD solutions. Because this method employs the simplest form derived from the Navier-Stokes equations describing the flow, all viscous and heat transfer factors are ignored. When the physical consequences of these assumptions are addressed, it is evident that skin friction drag, separation, and transonic shocks cannot be computed [35]. Panel approaches, on the other hand, have advantages over other computational aerodynamic methods, such as the vortex lattice method. While VLM models ignore thickness and apply boundary conditions (BCs) on an average mean surface, panel methods can model blunt geometries and apply BCs on the actual surface.

Panel methods can be briefly described as numerical schemes used to solve the linear, inviscid, irrotational flow equation at subsonic or supersonic freestream Mach numbers. The name of the equation that panel codes solve is the Prandtl-Giauert equation. For steady subsonic flow, this equation is usually can be defined as:

$$\tilde{\nabla}^2\phi = \left(1 - M_\infty^2\right)\phi_{xx} + \phi_{yy} + \phi_{zz} = 0 \tag{7}$$

For subsonic flows, Eq. (7) is elliptical. This type of equation allows any disturbance to be felt everywhere in the flow field, although the effect usually disappears with distance. To model the effect of the geometry on the flow, the singularities are distributed over the entire geometry, and their strengths are calculated over the surface velocity boundary conditions. The velocities induced by each ring vortex at a specified control point are calculated using the law of Biot-Savart. The contribution of each vortex loops and trailing wakes at a given i control point is calculated as follows:

$$\vec{V}_i = \sum_j^{\text{Loops}} \left[\vec{V}_{\text{loop}}\right]_j + \sum_j^{\text{Wakes}} \left[\vec{V}_{\text{wake}}\right]_j \tag{8}$$

Then freestream velocity component is added to the induced velocity and tangency boundary condition applied as:

$$\left[\vec{V}_\infty + \vec{V}_i\right] \cdot \hat{n}_i = 0 \tag{9}$$

In the panel method model, shade wakes are represented as vortex filaments that leave the sharp trailing edges of wings and possibly bodies. The strength of these filaments is determined by the Kutta condition, which allows the flow to leave the trailing edge properly. Also in VSPAERO, the location of these vortex filaments is solved iteratively in the overall flow field solution. Further details of the panel method algorithm can be found in the literature [36]. At the end of the process, the whole problem is reduced to the solution of a set of linear equations:

$$A\vec{x} = \vec{b} \tag{10}$$

where $\vec{x}$ represents the unknown circulation strengths. To reduce the computational cost, VSPAERO uses an iterative method, the generalized minimal residual method (GMRES), for the numerical solution of this system of linear equations.

$$\vec{R}_i = \vec{b} - A\vec{x}_i \tag{11}$$

where $\vec{R}_i \to \overrightarrow{0}$ as $i \to \infty$. Using the preconditioned GMRES algorithm, a matrix-free evaluation of the residual is obtained. In this application, the Precondition matrix was selected as an approximate LU decomposition of A. After calculating the strength of the singularities, the aerodynamic forces and moments affecting the geometry are obtained.

Various correction factors are used to take into account the local compressible effects that occur especially in the high-speed subsonic regime. The most popular of these is the Prandtl-Glauert rule, but a better model, the Karma-Tsien rule, is used in this study. In this model, the freestream Mach number is used to correct the pressure coefficient (C_p). It is defined as:

$$C_p = \frac{C_{p0}}{\sqrt{1 - M_\infty^2} + \left[M_\infty^2 / \left(1 + \sqrt{1 - M_\infty^2}\right)\right] C_{p0}/2} \tag{12}$$

where M_∞ is the freestream Mach number and C_{p0} is the potential flow coefficient of pressure. Since the panel method gives an inviscid solution, the parasite drag values are calculated with a semi-empirical approach.

2. Structural Mass Model

The most important parameter of an aircraft is undoubtedly its weight. Although a target MTOW is determined at the beginning of the design stage, the distribution of this weight to various components is also a critical issue. Because it is based on a primitive statistical technique, the accuracy of the aircraft weight estimation during the preliminary design phase is around %70-90. However, the estimation of this weight in relation to aerodynamic performance will be very important.

There are four main weight groups that make up a UAV's maximum take-off weight: empty weight, payload weight, and fuel weight. The total weight of the UAV is the sum of these three components:

$$W_{\text{MTOW}} = W_{\text{empty}} + W_{\text{payload}} + W_{\text{fuel}} \tag{13}$$

In these parameters, payload and fuel weight can be calculated from the requirements and engine selection. However, estimating the empty weight of the configuration to be created is an important issue. There are three major weight groups for the UAV empty weight:

$$W_{\text{empty}} = W_{\text{structure}} + W_{\text{engine}} + W_{\text{systems}} \tag{14}$$

In this equation, while the engine weight is obtained from the engine selection, the system and avionics weight can be approximately calculated from the requirements. The UAV structure weight is subdivided into four major weight groups:

$$W_{\text{structure}} = W_{\text{wing}} + W_{\text{tail}} + W_{\text{fuselage}} + W_{\text{gear}} \tag{15}$$

To model structural weight of the aircraft OpenVSP's structural module is used. The Structure Module in OpenVSP (Vehicle Sketch Pad) is a component of the software that allows users to create, analyze, and modify structural elements. It provides functionality for defining and manipulating various components, such as wings, fuselages, empennages, and other structural elements of an aircraft. Using a developed Python script ribs, spars, shells, and other structural elements are automatically created for each configuration. Structural weight calculation is performed by assigning default materials to these parts.

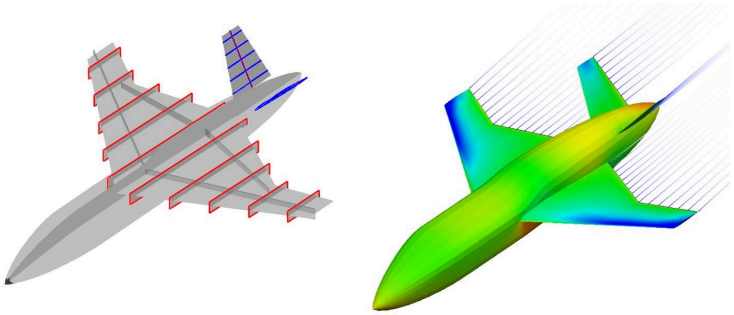

Fig. 3 Structural and aerodynamic models

3. Radar Cross Section Model

Radar Cross Section measures an object's detectability by radar systems. It denotes the effective area an object presents to an incident radar signal, reflecting the proportion scattered back to the radar receiver. Various parameters influence the radar cross-section, and these can be summarized as follows: the target's geometry, the materials it comprises, the frequency of the incident radar signal, the radar's polarization, and the positions of antennas relative to the target [37]. The definition of RCS is typically expressed in terms of electric fields, with the range R approaching infinity to ensure that the definition relies just on the target's characteristics.

$$\sigma = 4\pi \lim_{R\to\infty} \left(R^2 \frac{|\mathbf{E}^r|^2}{|\mathbf{E}^t|^2} \right) \tag{16}$$

where sigma is the RCS, R is the range, $|\mathbf{E}^r|$ and $|\mathbf{E}^t|^2$ are the backscattered and incident electric field squared magnitudes, respectively.

RCS is expressed in m^2 in physical scale and decibels referenced to a square meter (dBsm) in dB scale. The conversion between these two units is expressed as follows:

$$\sigma[\text{dBsm}] = 10\log(\sigma)\ [\text{m}^2] \tag{17}$$

Ray tracing techniques can be used to predict the RCS of objects by simulating the interaction of radar waves with the object's geometry, materials, and surface properties. By tracing the paths of the incident and reflected rays, and considering factors such as reflection, diffraction, and scattering, the RCS of the object can be estimated.

In this study, the RadarSimPy tool is used to calculate the radar cross-section of the generated concept configurations [38]. This Python module is integrated into the data generation script (see Figure 4). The STL file, which consists of unstructured triangulated surfaces of concept configurations created through the Python API, is used as an input geometry to the RadarSimPy code. In this way, it is ensured that the RCS value of each configuration is obtained with high performance. The algorithm can calculate the monostatic radar cross section of the aerial vehicles for the given signal parameters.

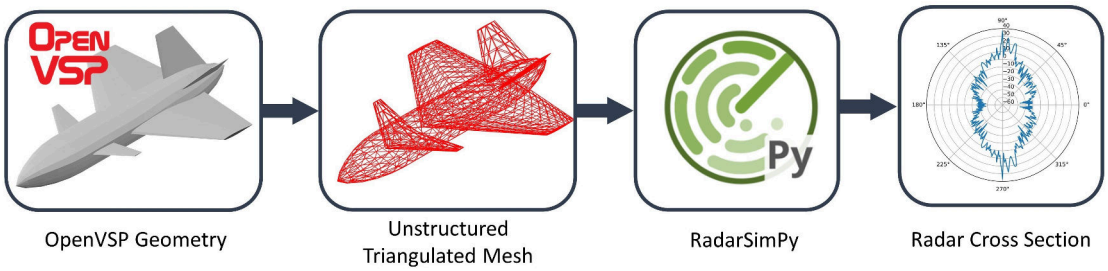

Fig. 4 RCS calculation of configurations

D. AI-based Surrogate Models

In this part, AI-based surrogate models of aircraft performance models will be built. Thus, the performance of the generated configurations can be calculated without the need for analysis. A large number of configurations were produced using the framework first developed for this purpose. The Latin hypercube sampling (LHS) was added to the algorithm to generate a quasi-random sampling distribution [39]. Thanks to this algorithm, it is possible to cover all design space with a limited data point. Design and flow variables used in data generation are given in Table 2.

Neural network algorithms were used to train the black box model. We utilize an essential multi-layer perceptron structure to regress the performance data, Y, using X. For a fully-connected network with L hidden layers, this amounts to the following modeling equations relating the input features x, to its target prediction y. A generic structure of a deep neural network consisting of a multilayer perceptron with M input features and N layers. It is composed of sequentially connected layers, which comprise sets of neurons that are combinations of mathematical operations followed by nonlinear activation functions. The model parameters ξ are defined as $\xi = \{W, b\}$, where $W = \{w_i\}_{i=1}^{N}$, and $b = \{b_i\}_{i=1}^{N}$. The output of the lth layer is:

$$f(x, \xi_l) = f_{w_l, b_l}(x) = z_l \left(\sum_{j=1}^{N_l} w_{lj} x_j + b_l \right) \tag{18}$$

$$= Z_l \left(w_l^T x_l + b_l \right) \quad (l = 1, \ldots, N) \tag{19}$$

where N_t is the neuron number and Z_l is a nonlinear activation function of a specific lth layer, and x_l is the input of the lth layer and also the output of the $(l-1)$th layer. In addition to this, w_l and b_l are learnable parameters and called

Table 2 Design and flow variables for the UAV conceptual design space exploration

	Parameter	Variable	Units
Wing	Wing Area	S	m^2
	Aspect Ratio	AR	~
	Span	b	m
	Chord	c	m
	Taper Ratio	λ	~
	Sweep	Λ	deg
Fuselage	Diameter	d	m
	Length	L	m
Flow Condition	Angle of Attack	α	deg
	Mach Number	M	~

weight and bias terms of that layer respectively. Finally, the output of the last layer is a result of the composite and complex mapping defined as:

$$\hat{y}(x) := \left(f_{w_n,b_n} \circ \cdots \circ f_{w_1,b_1}\right)(x) \tag{20}$$

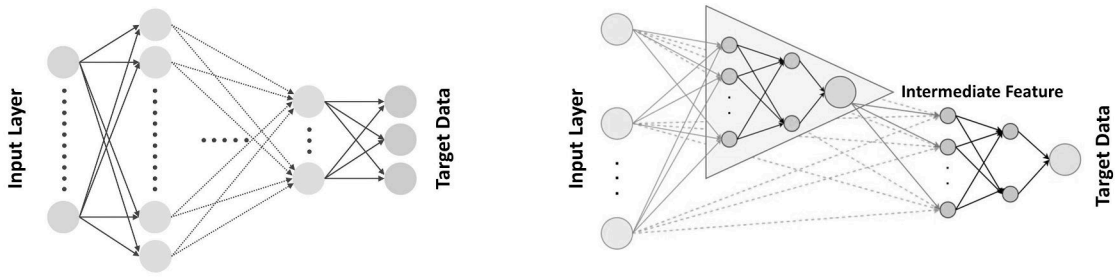

Fig. 5 Neural-network and cascaded neural-network architecture for aircraft performance prediction

This work also proposes a cascaded neural network architecture for estimating aerodynamic performance data. The architecture depicted in Figure 5 is a single neural network consisting of two parts: The first part estimates the intermediate features:

$$\hat{y}_{int} := \left(f^{[1]}_{w_n,b_n} \circ \cdots \circ f^{[1]}_{w_1,b_1}\right)(x) \tag{21}$$

where $\hat{y}_{int}$ represents C_L for the drag coefficient. Then, we concatenate the intermediate feature to the main feature set and provide this new input to the second part of the neural network, where we estimate the output variable. Note that these two parts of the neural network are not trained separately. All trainable parameters in both parts are updated simultaneously at each mini-batch.

$$x_{int} = \{x, \hat{y}_{int}\} \tag{22}$$

$$\hat{y} := \left(f^{[2]}_{w_n,b_n} \circ \cdots \circ f^{[2]}_{w_1,b_1}\right)(x_{int}) \tag{23}$$

The customized neural network architecture aims to increase the accuracy of drag estimation by incorporating additional information about C_L, which has a high correlation with this parameter. To address this issue, we introduce an intermediate estimator to provide the neural network with additional information about this variable. As the loss in the intermediate estimator decreases, the accuracy of the main output is expected to increase further. The inclusion of this additional information enables the neural network to better capture the underlying relationships between performance data and geometry and flow condition information, resulting in a more accurate estimation of the drag coefficient.

E. Multi-Objective Genetic Algorithm

In this layer, a genetic algorithm (GA) based optimization runs using AI-driven aerodynamic performance, structural mass, and radar cross section prediction. In the GA approach, an initial set of designs is generated using design variables remaining within predetermined limits [40]. For each design, fitness values are calculated using the cost function, and a random subset is selected from the current design set for those that better fit. Random operations are used to create new designs using the subset of selected designs. A multi-objective genetic algorithm (MOGA) is an optimization method designed for problems with multiple conflicting objectives. It extends the traditional genetic algorithm to simultaneously optimize diverse criteria. In a MOGA, a population of potential solutions evolves through genetic operations, aiming to discover a set of solutions along the Pareto front, a trade-off curve, where enhancing one objective may compromise another. This approach allows decision-makers to explore a diverse range of optimal solutions, providing valuable insights into the complex trade-offs inherent in multi-objective optimization problems across various domains.

In the optimization cycle, it is possible to scan huge design space in seconds by using the network-based black box functions given below:

- The performance of an aircraft is mainly related to geometry, flow direction, Reynolds number and Mach number. For the main performance parameters, lift (C_L) and drag coefficients (C_D), this relationship can be expressed as follows:

$$C_{L,D} = f_{aero}(Geometry, \alpha, \mathrm{Re}, M) \tag{24}$$

- The mass model includes the engine, avionics, payload, fuel, and structural weight. AI-based structural weight estimation is given as:

$$W_{str} = f_{structural}(Geometry, \alpha, \mathrm{Re}, M) \tag{25}$$

- The RCS value of an aircraft is mainly related to geometry and surface material. For this study, we only considered the effect of geometry, and the black box model only takes this as input.

$$RCS = f_{rcs}(Geometry) \tag{26}$$

At the end of the process, each concept is optimized for given objective functions such as maximizing efficiency while minimizing structural weight and radar cross section.

III. Application of the Model

In this section, a medium-sized high subsonic UAV is designed according to the given performance requirements using the developed algorithm. Concept configurations of this UAV are given in Fig. 7. The purpose of this optimization problem is to obtain a configuration with maximum efficiency and minimum radar cross section and structural weight.

The optimization problem can be defined as:

$$\underset{x}{\text{minimize}} \quad \left\{ f_1(x) = \frac{1}{L/D}, \quad f_2(x) = W_{str}, \quad f_3(x) = RCS \right\} \tag{27}$$

$$\text{subject to} \quad 0.30 < C_L < 0.33 \tag{28}$$

$$C_D < 0.03 \tag{29}$$

$$RCS < 0.2 \tag{30}$$

where x includes the cruise angle of attack, wing aspect ratio, taper ratio, and sweep angle. The limits of these variables are given in Table 3.

Table 3 Wing design variables and limits

Variables	Min	Max
Cruise AoA	0	4
AR	3	7
Taper	0.1	0.6
Sweep	0	30

For this study, the first surrogate models of UAV performance models were created. Design space was discovered using these black-box models. In Figure 6, predicted and real Lift Coefficient, Drag Coefficient, Empty Weight, RCS parameters are given. In these graphs, the accuracy of approximately 1000 configurations under different flow conditions can be observed.

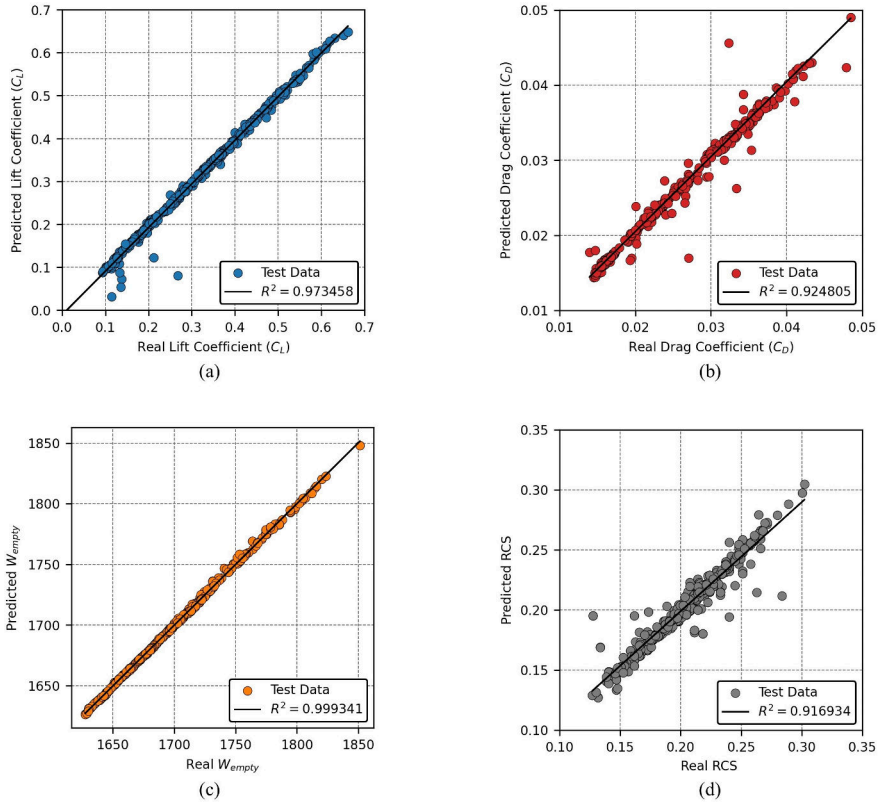

Fig. 6 Performance of black-box models: (a) Lift Coefficient, (b) Drag Coefficient, (c) Empty Weight, (d) RCS

After the optimization cycle, optimized versions of each concept configuration are presented to the user. As can be seen from Figure 7, the initial layout and size of the traditional, lambda, and delta configurations have been determined. Thanks to the algorithm, aerodynamic, structural, and RCS performance parameters were also obtained in detail.

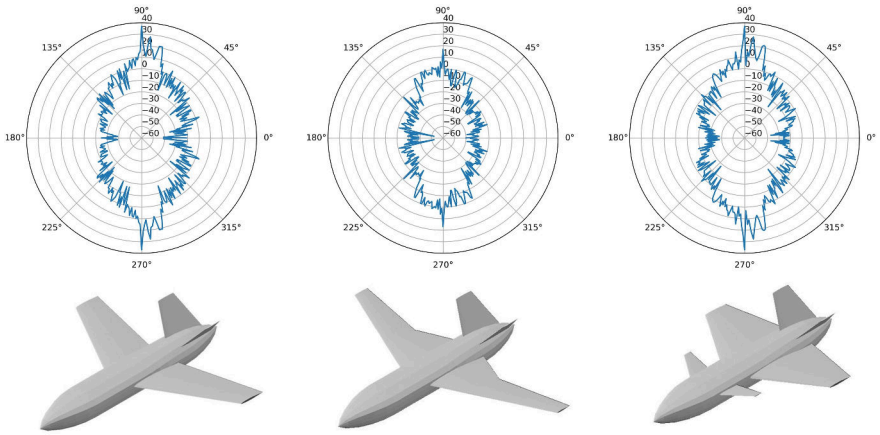

Fig. 7 Conventional, Lambda, and Delta configuration concepts with RCS values in dBsm

IV. Conclusion

In conclusion, this paper has successfully introduced and implemented an intelligent conceptual design algorithm aimed at bringing numerical data into the early stages of the design process while significantly reducing the dependence on human intervention. The developed algorithm not only helps the selection of optimal concept configurations but also streamlines the initial sizing process. Using AI-driven algorithms, our approach demonstrates a remarkable decrease in computational time, marking a transformative shift in the efficiency of the design process. By automating critical aspects of conceptual design, our method contributes to cost reduction and accelerates the decision-making timeline. Moving forward, the integration of AI-driven surrogate models and optimization loops holds promising potential for advancing multidisciplinary design methodologies.

Acknowledgments

Hasan Karali is co-funded by the EPSRC and the BAE Systems under 210085 numbered Industrial CASE award : *Towards Trustworthy AI-driven Autonomous Systems: Multi-Disciplinary Design Optimisation*.

References

[1] Humphreys, C., Cobb, R., Jacques, D., and Reeger, J., "Optimal mission path for the uninhabited loyal Wingman," *16th AIAA/ISSMO Multidisciplinary Analysis and Optimization Conference*, 2015, p. 2792.

[2] Stensrud, R., Mikkelsen, B., Betten, S., and Valaker, S., "A proposal for a simple evaluation method in support of the initial concept phase assessing a future unmanned Loyal Wingman for Royal Norwegian Air Force (RNoAF)," *38th International Symposium on Military Operational Research (38 ISMOR)*, 2021.

[3] Harper, J., "The Rise of Skyborg: Air Force Betting on New Robotic Wingman," *National Defense*, 2020. URL https://www.nationaldefensemagazine.org/articles/2020/9/25/air-force-betting-on-new-robotic-wingman.

[4] Gunzinger, M., and Autenried, L., "Understanding the Promise of Skyborg and Low-Cost Attritable Unmanned Aerial Vehicles," *Mitchell Institute Policy Paper*, Vol. 24, 2020.

[5] Reim, G., "Analysis: US Air Force eyes adoption of 'Loyal Wingman' UAVs," *Flight Global*, 2018. URL https://www.flightglobal.com/analysis/analysis-us-air-force-eyes-adoption-of-loyal-wingman-uavs/129330.article.

[6] Smith, A., and Rogers, M., 2021. URL https://www.gao.gov/products/gao-21-439.

[7] Colombi, J., Bentz, B., Recker, R., Lucas, B., and Freels, J., "Attritable design trades: Reliability and cost implications for unmanned aircraft," *2017 Annual IEEE International Systems Conference (SysCon)*, IEEE, 2017, pp. 1–8.

[8] Pittaway, N., "Boeing details MQ-28A payload ground test phase," *Australian Defence Magazine*, 2022. URL https://www.australiandefence.com.au/defence/air/boeing-details-mq-28a-payload-ground-test-phase.

[9] Newdick, T., "The United Kingdom Has Chosen Who Will Build Its First Prototype Loyal Wingman Combat Drone," *The Drive The Warzone*, 2021. URL https://www.thedrive.com/the-war-zone/38898/the-united-kingdom-has-chosen-who-will-build-its-first-prototype-loyal-wingman-combat-drone.

[10] Sobieszczanski-Sobieski, J., "Multidisciplinary design optimization: an emerging new engineering discipline," *Advances in structural optimization*, Springer, 1995, pp. 483–496.

[11] Nguyen, N.-V., Choi, S.-M., Kim, W.-S., Lee, J.-W., Kim, S., Neufeld, D., and Byun, Y.-H., "Multidisciplinary unmanned combat air vehicle system design using multi-fidelity model," *Aerospace Science and Technology*, Vol. 26, No. 1, 2013, pp. 200–210.

[12] Karali, H., Inalhan, G., Umut Demirezen, M., and Adil Yukselen, M., "A new nonlinear lifting line method for aerodynamic analysis and deep learning modeling of small unmanned aerial vehicles," *International Journal of Micro Air Vehicles*, Vol. 13, 2021, p. 17568293211016817.

[13] Ng, L. W., and Willcox, K. E., "Multifidelity approaches for optimization under uncertainty," *International Journal for numerical methods in Engineering*, Vol. 100, No. 10, 2014, pp. 746–772.

[14] Brunton, S. L., Nathan Kutz, J., Manohar, K., Aravkin, A. Y., Morgansen, K., Klemisch, J., Goebel, N., Buttrick, J., Poskin, J., Blom-Schieber, A. W., et al., "Data-driven aerospace engineering: reframing the industry with machine learning," *AIAA Journal*, Vol. 59, No. 8, 2021, pp. 2820–2847.

[15] AIAA Digital Engineering Integration Committee, "Digital Twin: Definition & Value—An AIAA and AIA Position Paper," *AIAA: Reston, VA, USA*, 2020.

[16] Dantas de Jesus Ferreira, J. A., and Secco, N. R., "Decision tree classifiers for unmanned aircraft configuration selection," *Aircraft Engineering and Aerospace Technology*, Vol. 93, No. 6, 2021, pp. 1122–1132.

[17] Ahn, J., Kim, H.-J., Lee, D.-H., and Rho, O.-H., "Response surface method for airfoil design in transonic flow," *Journal of Aircraft*, Vol. 38, No. 2, 2001, pp. 231–238. https://doi.org/10.2514/2.2780.

[18] Andres-Perez, E., Carro-Calvo, L., Salcedo-Sanz, S., and Martin-Burgos, M. J., "Aerodynamic shape design by evolutionary optimization and support vector machines," *Springer Tracts in Mechanical Engineering*, Springer, Cham, 2016, pp. 1–24. https://doi.org/10.1007/978-3-319-21506-8_1.

[19] Han, Z., Zhang, K., Song, W., and Liu, J., "Surrogate-based aerodynamic shape optimization with application to wind turbine airfoils," *American Institute of Aeronautics and Astronautics*, 2013. https://doi.org/10.2514/6.2013-1108.

[20] Xu, J., Han, Z., Yan, X., and Song, W., "Aerodynamic design of megawatt wind turbine blades with NPU-WA airfoils," *IOP Conference Series: Earth and Environmental Science*, Vol. 495, 2020, p. 012018. https://doi.org/10.1088/1755-1315/495/1/012018.

[21] Li, J., Bouhlel, M. A., and Martins, J. R. R. A., "Data-based approach for fast airfoil analysis and optimization," *AIAA Journal*, Vol. 57, 2019, pp. 581–596. https://doi.org/10.2514/1.J057129.

[22] Du, X., and Leifsson, L., "Optimum aerodynamic shape design under uncertainty by utility theory and metamodeling," *Aerospace Science and Technology*, Vol. 95, 2019, p. 105464. https://doi.org/10.1016/j.ast.2019.105464.

[23] Lin, Q., Chen, C., Xiong, F., Chen, S., and Wang, F., "An Improved PC-Kriging Method for Efficient Robust Design Optimization," *Conference on Control and Automation*, 2020, pp. 394–411. https://doi.org/10.1007/978-981-32-9941-2_33.

[24] Nagawkar, J., and Leifsson, L., "Applications of polynomial chaos-based cokriging to simulation-based analysis and design under uncertainty," *46th Design Automation Conference*, 2020.

[25] Bouhlel, M. A., He, S., and Martins, J. R. R. A., "Scalable gradient-enhanced artificial neural networks for airfoil shape design in the subsonic and transonic regimes," *Structural and Multidisciplinary Optimization*, Vol. 61, 2020, pp. 1363–1376. https://doi.org/10.1007/s00158-020-02488-5.

[26] Du, X., He, P., and Martins, J. R. R. A., "A B-spline-based generative adversarial network model for fast interactive airfoil aerodynamic optimization," *AIAA SciTech Forum*, AIAA, Orlando, FL, 2020. https://doi.org/10.2514/6.2020-2128.

[27] Barnhart, S. A., Narayanan, B., and Gunasekaran, S., "Blown wing aerodynamic coefficient predictions using traditional machine learning and data science approaches," *AIAA SciTech Forum*, 2021. https://doi.org/10.2514/6.2021-0616.

[28] Yu, B., Xie, L., and Wang, F., "An improved deep convolutional neural network to predict airfoil lift Coefficient," *Proceedings of the International Conference on Aerospace System Science and Engineering 2019*, Springer Singapore, Singapore, 2020, pp. 275–286.

[29] Zhang, Y., Sung, W. J., and Mavris, D. N., "Application of convolutional neural network to predict airfoil lift coefficient," *2018 AIAA/ASCE/AHS/ASC Structures, Structural Dynamics, and Materials Conference*, American Institute of Aeronautics and Astronautics, 2018. https://doi.org/10.2514/6.2018-1903.

[30] Sadraey, M. H., *Aircraft design: A systems engineering approach*, Aerospace Series, John Wiley and Sons, Chichester, 2013. https://doi.org/10.1002/9781118352700, URL http://doi.org/10.1002/9781118352700.

[31] Roskam, J., and Lan, C.-T. E., *Airplane aerodynamics and performance*, DARcorporation, 1997.

[32] Garcia, J. A., Bowles, J. V., Kinney, D. J., Melton, J. E., and Jiang, X. J., "VIPER Integrated MDAO Analysis for Conceptual Design of Supersonic X-Plane Vehicles," Tech. rep., 2019.

[33] McDonald, R. A., "Advanced modeling in OpenVSP," *16th AIAA Aviation Technology, Integration, and Operations Conference*, 2016, p. 3282.

[34] McDonald, R. A., and Gloudemans, J. R., "Open Vehicle Sketch Pad: An Open Source Parametric Geometry and Analysis Tool for Conceptual Aircraft Design," *AIAA SCITECH 2022 Forum*, 2022, p. 0004.

[35] Erickson, L. L., "Panel methods: An introduction," Tech. rep., 1990.

[36] Katz, J., and Plotkin, A., *Low-speed aerodynamics*, Vol. 13, Cambridge university press, 2001.

[37] Karakoc, A., and Kaya, H., "A multi-objective multi-disciplinary optimization approach for NATO AVT 251 UCAV–MULDICON," *2018 Applied Aerodynamics Conference*, 2018, p. 3001.

[38] Peng, Z., "rookiepeng/radarsimpy:," , Jul 2022. https://doi.org/10.5281/zenodo.6792269.

[39] Bouhlel, M. A., Hwang, J. T., Bartoli, N., Lafage, R., Morlier, J., and Martins, J. R. R. A., "A Python surrogate modeling framework with derivatives," *Advances in Engineering Software*, 2019, p. 102662. https://doi.org/https://doi.org/10.1016/j.advengsoft.2019.03.005.

[40] Chipperfield, A., and Fleming, P., "The MATLAB genetic algorithm toolbox," 1995.

2024-01-04

AI-driven multidisciplinary conceptual design of unmanned aerial vehicles

Karali, Hasan

AIAA

Karali H, Inalhan G, Tsourdos A. (2024) AI-driven multidisciplinary conceptual design of unmanned aerial vehicles. In: AIAA SCITECH 2024 Forum, 8-12 January 2024, Orlando, Florida. Paper number AIAA 2024-1708

https://doi.org/10.2514/6.2024-1708